Fabrication and characterization of machined multi-core fiber tweezers for single cell manipulation

Research Article | Vol. 26, No. 3 | 5 Feb 2018 | OPTICS EXPRESS 3557
Optics EXPRESS

Fabrication and characterization of machined multi-core fiber tweezers for single cell manipulation

GEORGIA ANASTASIADI,[1,*] MARK LEONARD,[2] LYNN PATERSON,[3] AND WILLIAM N. MACPHERSON[1]

[1]*Institute of Photonics and Quantum Sciences, School of Engineering and Physical Sciences, Heriot-Watt University, Edinburgh, EH14 4AS, UK*
[2]*Institute of Signals, Sensors and Sciences, School of Engineering and Physical Sciences, Heriot-Watt University, Edinburgh, EH14 4AS, UK*
[3]*Institute of Biological Chemistry, Biophysics and Bioengineering, School of Engineering and Physical Sciences, Heriot-Watt University, Edinburgh, EH14 4AS, UK*
**ga10@hw.ac.uk*
www.aop.hw.ac.uk

Abstract: Optical tweezing is a non-invasive technique that can enable a variety of single cell experiments; however, it tends to be based on a high numerical aperture (NA) microscope objective to both deliver the tweezing laser light and image the sample. This introduces restrictions in system flexibility when both trapping and imaging. Here, we demonstrate a novel, high NA tweezing system based on micro-machined multicore optical fibers. Using the machined, multicore fiber tweezer, cells are optically manipulated under a variety of microscopes, without requiring a high NA objective lens. The maximum NA of the fiber-based tweezer demonstrated is 1.039. A stable trap with a maximum total power 30 mW has been characterized to exert a maximum optical force of 26.4 pN, on a trapped, 7 μm diameter yeast cell. Single cells are held 15-35 μm from the fiber end and can be manipulated in the x, y and z directions throughout the sample. In this way, single cells are controllably trapped under a Raman microscope to categorize the yeast cells as live or dead, demonstrating trapping by the machined multicore fiber-based tweezer decoupled from the imaging or excitation objective lens.

OCIS codes: (350.4855) Optical tweezers or optical manipulation; (060.2280) Fiber design and fabrication; (140.7010) Laser trapping; (170.5660) Raman spectroscopy.

References and links

1. A. Ashkin, J. M. Dziedzic, J. E. Bjorkholm, and S. Chu, "Observation of a single-beam gradient force optical trap for dielectric particles," Opt. Lett. **11**(5), 288–290 (1986).
2. O. M. Maragò, P. H. Jones, P. G. Gucciardi, G. Volpe, and A. C. Ferrari, "Optical trapping and manipulation of nanostructures," Nat. Nanotechnol. **8**(11), 807–819 (2013).
3. R. Ghadiri, T. Weigel, C. Esen, and A. Ostendorf, "Microassembly of complex and three-dimensional microstructures using holographic optical tweezers," J. Micromech. Microeng. **22**(6), 065016 (2012).
4. K. C. Neuman, E. H. Chadd, G. F. Liou, K. Bergman, and S. M. Block, "Characterization of Photodamage to Escherichia coli in Optical Traps," Biophys. J. **77**(5), 2856–2863 (1999).
5. A. Constable, J. Kim, J. Mervis, F. Zarinetchi, and M. Prentiss, "Demonstration of a fiber-optical light-force trap," Opt. Lett. **18**(21), 1867–1869 (1993).
6. P. R. T. Jess, V. Garcés-Chávez, D. Smith, M. Mazilu, L. Paterson, A. Riches, C. S. Herrington, W. Sibbett, and K. Dholakia, "Dual beam fibre trap for Raman micro-spectroscopy of single cells," Opt. Express **14**(12), 5779–5791 (2006).
7. J. Guck, R. Ananthakrishnan, H. Mahmood, T. J. Moon, C. C. Cunningham, and J. Käs, "The Optical Stretcher: A Novel Laser Tool to Micromanipulate Cells," Biophys. J. **81**(2), 767–784 (2001).
8. T. Kolb, S. Albert, M. Haug, and G. Whyte, "Optofluidic rotation of living cells for single-cell tomography," J. Biophoton. **8**(3), 239–246 (2015).

#315524 https://doi.org/10.1364/OE.26.003557
Journal © 2018 Received 13 Dec 2017; revised 18 Jan 2018; accepted 18 Jan 2018; published 1 Feb 2018

Optics EXPRESS

9. M. Boerkamp, T. van Leest, J. Heldens, A. Leinse, M. Hoekman, R. Heideman, and J. Caro, "On-chip optical trapping and Raman spectroscopy using a TripleX dual-waveguide trap," Opt. Express **22**(25), 30528–30537 (2014).
10. K. Taguchi, K. Atsuta, T. Nakata, and M. Ikeda, "Single laser beam fiber optic trap," Opt. Quantum Electron. **33**(1), 99–106 (2001).
11. R. Taylor and C. Hnatovsky, "Particle trapping in 3-D using a single fiber probe with an annular light distribution," Opt. Express **11**(21), 2775–2782 (2003).
12. Z. Liu, C. Guo, J. Yang, and L. Yuan, "Tapered fiber optical tweezers for microscopic particle trapping: fabrication and application," Opt. Express **14**(25), 12510–12516 (2006).
13. C. Liberale, P. Minzioni, F. Bragheri, F. De Angelis, E. Di Fabrizio, and I. Cristiani, "Miniaturized all-fiber probe for three-dimensional optical trapping and manipulation," Nat. Photonics **1**(12), 723–727 (2007).
14. C. Liberale, G. Cojoc, F. Bragheri, P. Minzioni, G. Perozziello, R. La Rocca, L. Ferrara, V. Rajamanickam, E. Di Fabrizio, and I. Cristiani, "Integrated microfluidic device for single-cell trapping and spectroscopy," Sci. Rep. **3**(1), 1258 (2013).
15. L. Yu, S. Mohanty, G. Liu, S. Genc, Z. Chen, and M. W. Berns, "Quantitative phase evaluation of dynamic changes on cell membrane during laser microsurgery," J. Biomed. Opt. **13**(5), 050508 (2008).
16. S. R. Ribeiro, R. Queirós, O. Soppera, A. Guerreiro, and P. A. S. Jorge, "Optical Fiber Tweezers Fabricated by Guided Wave Photo-Polymerization," Photonics **2**(2), 634–645 (2015).
17. T. Čižmár and K. Dholakia, "Shaping the light transmission through a multimode optical fibre: complex transformation analysis and applications in biophotonics," Opt. Express **19**(20), 18871–18884 (2011).
18. I. T. Leite, S. Turtaev, X. Jiang, M. Šiler, A. Cuschieri, P. S. J. Russell, and T. Čižmár, "Three-dimensional holographic optical manipulation through a high-numerical-aperture soft-glass multimode fiber," Nat. Photonics **11**(12), 33 (2017).
19. S. Bianchi and R. Di Leonardo, "A multi-mode fiber probe for holographic micromanipulation and microscopy," Lab Chip **12**(3), 635–639 (2012).
20. X. Xue, W. Zhang, L. Yin, S. Wei, S. Gao, P. Geng, and J. Ruan, "All-fiber intermodal Mach–Zehnder interferometer based on a long-period fiber grating combined with a fiber bitaper," Opt. Commun. **285**(19), 3935–3938 (2012).
21. L. Yuan, Z. Liu, J. Yang, and C. Guan, "Twin-core fiber optical tweezers," Opt. Express **16**(7), 4559–4566 (2008).
22. A. L. Barron, A. K. Kar, and H. T. Bookey, "Dual-beam interference from a lensed multicore fiber and its application to optical trapping," Opt. Express **20**(21), 23156–23161 (2012).
23. G. M. H. Flockhart, W. N. MacPherson, J. S. Barton, J. D. C. Jones, L. Zhang, and I. Bennion, "Two-axis bend measurement with Bragg gratings in multicore optical fiber," Opt. Lett. **28**(6), 387–389 (2003).
24. G. Anastasiadi, L. Paterson, and W. N. MacPherson, "Machined multicore optical fibers for on -chip optical manipulation," Proc. SPIE **10347**, 1034702 (2017).
25. S. F. Tolić-Nørrelykke, E. Schäffer, J. Howard, F. S. Pavone, F. Jülicher, and H. Flyvbjerg, "Calibration of optical tweezers with positional detection in the back focal plane," Rev. Sci. Instrum. **77**(10), 103101 (2006).
26. P. Minzioni, F. Bragheri, C. Liberale, E. Di Fabrizio, and I. Cristiani, "A Novel Approach to Fiber-Optic Tweezers: Numerical Analysis of the Trapping Efficiency," IEEE J. Sel. Top. Quantum Electron. **14**(1), 151–157 (2008).
27. N. Malagnino, G. Pesce, A. Sasso, and E. Arimondo, "Measurements of trapping efficiency and stiffness in optical tweezers," Opt. Commun. **214**(1-6), 15–24 (2002).
28. Y. Liu and M. Yu, "Investigation of inclined dual-fiber optical tweezers for 3D manipulation and force sensing," Opt. Express **17**(16), 13624–13638 (2009).
29. H. Cabrera, J. J. Suárez-Vargas, A. López, H. Núñez, G. Carvalho, G. Coceano, and D. Cojoc, "Experimental determination of trapping efficiency of optical tweezers," Philos. Mag. Lett. **93**(11), 655–663 (2013).
30. A. Ashkin, "Forces of a single-beam gradient laser trap on a dielectric sphere in the ray optics regime," Biophys. J. **61**(2), 569–582 (1992).
31. L. Allen, M. W. Beijersbergen, R. J. C. Spreeuw, and J. P. Woerdman, "Orbital angular momentum of light and the transformation of Laguerre-Gaussian laser modes," Phys. Rev. A **45**(11), 8185–8189 (1992).
32. N. B. Simpson, D. McGloin, K. Dholakia, L. Allen, and M. J. Padgett, "Optical tweezers with increased axial trapping efficiency," J. Mod. Opt. **45**(9), 1943–1949 (1998).
33. C. Xie, D. Chen, and Y. Q. Li, "Raman sorting and identification of single living micro-organisms with optical tweezers," Opt. Lett. **30**(14), 1800–1802 (2005).
34. Z. Movasaghi, S. Rehman, and I. U. Rehman, "Raman Spectroscopy of Biological Tissues," Appl. Spectrosc. Rev. **42**(5), 493–541 (2007).

1. Introduction: fiber-based optical tweezers

Since its first demonstration by Ashkin *et al.* in 1986 [1], optical tweezing has become a powerful tool to manipulate micro- or nano-particles. Optical tweezers (OT) have seen widespread use for particle confinement [2], building microstructures [3], and force spectroscopy [4]. However, the traditional high numerical aperture (NA) configuration suffers

Optics EXPRESS

from a lack of system flexibility due to the requirement to direct the trapping beam through the high NA objective lens in order to form a tightly focused laser beam trap. This limits its usefulness in many cases. For example, trapping in thick samples is limited due to spherical aberrations in the optical trap occurring at depth resulting in a much-reduced trapping force. Trapping through turbid media, where it is difficult to form a high intensity focus because the beam is scattered before it reaches the trapping region, is problematic. The requirement for a high NA lens also restricts the field of view: larger fields of view can only be achieved by precisely aligning a lower NA imaging objective, co-axially with the high NA tweezing objective on the opposite side of a thin sample, creating an extremely restricted volume for positioning and moving the sample stage. There is additional interest in decoupling trapping optics from imaging optics as many commercial imaging systems do not lend themselves to having tweezing optics incorporated into the imaging path so it is challenging to perform particle or cell trapping using facility-based microscopes.

The development in the 1990's of optical fiber-based tweezing systems overcame some of these restrictions by delivering the trapping light into the sample via fibers as an alternative to high NA optics in the imaging path. The first fiber trap was demonstrated by Constable *et al* [5] where two opposed fibers were used to trap a particle. Here the beam profile traps the particle along the optical path and the particle position can be held stable when the optical forces are balanced along the optical axis. This has found niche applications in Raman trapping [6], cell stretching [7] and cell rotation [8]. However, this approach demands precise alignment of the two fibers and careful microfluidic flow control of the sample. Integrated waveguides have been shown to overcome alignment problems [9] but do not offer full 3D manipulation. Taguchi *et al* [10] demonstrated 2D trapping in the weakly focused beam emitted from a single fiber which was polished to a tapered, spherical end with a radius of several micrometres. The first report of 3D trapping using a single fiber was by Taylor and Hnatovsky [11] who used a partially metalized, hollow-tipped, tapered fiber probe fabricated by selective chemical etching. The force produced by the light pressure from the resulting annular beam was balanced by an electrostatic force towards the tip thereby creating a stable 3D trap. Single fibers have been further refined using heating and drawing of a single core fiber to form a tapered tip able to focus the light and optically trap particles in 3D [12]. However, in these cases, the trapping position was reported to be very close (~1 μm) to the fiber end and this restricts the range of potential applications.

A significant development for fiber laser traps was to fabricate beam steering mirrors onto the fiber-end. The first example of this was presented by Liberale *et al.* [13]. Here, four optical fibers containing beam steering mirrors are glued together to form a probe that could trap a polystyrene microbead in 3 dimensions, 35 μm from the end face. However, this design demands high precision in terms of alignment and manufacturing, and results in a probe with near millimeter scale dimensions. A further development was to fabricate micro-prism reflectors on the end facet of a fiber bundle using two-photon lithography [14]. Similar to [13] a particle or cell could be trapped where the beams converged. Other methods to modify fiber tips to enable tweezing include fabrication of axicon tips, used to both trap and lyse mammalian cells using CW and ultrafast light, respectively [15] and on-tip polymerization using a guided wave [16]. More recent research on optical trapping using multimode optical fibers has been demonstrated by Cizmar *et al.* [17, 18] to trap particles using both static and dynamic intensity patterns, and similarly by Leonardo *et al.*, to transmit digital holograms that can optically trap fluorescent beads of 2 μm in 2D as well as image the sample [19].

In this paper, we show fabrication and use of a flexible, single fiber-based optical tweezer, of only 150 μm diameter, with a NA between 0.94 and 1.039, created by forming end face mirrors using focused ion beam (FIB) milling of two cores in a multicore fiber. The fiber tweezer is capable of 3D optical manipulation under a variety of inspection microscopes.

Optics EXPRESS

2. Multicore optical fiber-based tweezer: design and fabrication

2.1 Single fiber-based tweezer design

We have used multicore optical fiber (MCF) as the basis of a fiber tweezer due to its annular distribution of light and its small diameter of 150 µm with distance between diagonal cores of 65 µm, as seen in Fig. 1(a), which makes it suitable for integration with 'lab on a chip' devices. MCF consists of 2 or more cores, typically assembled by creating a preform with multiple cores that is then drawn into a single multicore fiber. Recent exploitation of MCFs include polishing and bi-tapering of the fiber to create a Mach–Zehnder interferometer [20], a twin-core fiber–based optical tweezer produced by tapering the fiber which was shown to trap particles very close to the tip end [21] and a lensed four core fiber that could trap particles in one dimension [22].

In order to create a *stable*, 3D optical trap at the end of a *single* fiber, as opposed to a fiber bundle, or a weak trap at the end of a tapered fiber, we use a multicore fiber, as shown in Fig. 1(a). We cut mirrors of angle θ into two diagonally opposite cores at the fiber-end as shown in Fig. 1(b), a similar arrangement to that used by Liberale *et al.* in the four fiber bundle [13].

The mirror angle (θ) with respect to the core axis has to be slightly larger than the critical angle so that the core-guided beams undergo total internal reflection (TIR) at the mirror-media interface as depicted in Fig. 1(b). After refraction at the fiber/media interface the beams converge to form a trapping region several to tens of micrometres away (d_{trap}) from the fiber-end. Angle θ_{prop} is defined as the propagation angle with respect to the fiber end-face and angle φ as the propagation angle with respect to the fiber axis. An illustration of the converging beams is shown in Fig. 1(c). The fiber consists of four silica cores of refractive index 1.469 ± 0.004 as measured by interferometry and doped silica cladding of refractive index 1.463 based upon the refractive index profile of a conventional SMF 28 fiber. When the fiber is immersed in water, the critical angle is calculated to be 64.79°.

The tweezing system described in this paper uses the same geometry, based on TIR, as Liberale *et al.* [13]. Using MCF as opposed to a four fiber bundle, the distance between the two diagonal cores in reduced by almost half thus reducing the overall diameter of the fiber tweezer from 360 µm to 150 µm. In addition, by using MCF, the assembly of the fiber tweezer is more straightforward as we do not have the pre-assembly step of gluing four fibers together within a glass capillary or the facet polishing step prior to FIB machining. Whilst the single fiber tweezer presents advantages in terms of smaller size and easier assembly, the overall cost of fabrication is similar because FIB milling is the major cost in the process. FIB offers excellent precision, ideal for prototyping and proof of concept demonstrations. However, other mirror fabrication techniques, such as laser machining or mechanical polishing, may offer routes for up-scaled production.

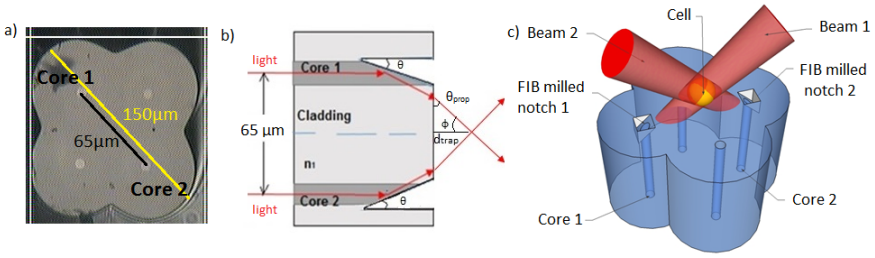

Fig. 1. a) Micrograph of the four-core fiber end-face. Diagonally opposite cores, 65 µm apart, are machined to form the steering mirrors, b) Cross-section of the fiber tweezer design. Light propagates along the core and undergoes TIR at the mirror/media interface followed by refraction at the fiber/media interface. The light from the two diagonally opposite cores converge at a distance d_{trap} from the fiber-end, c) 3D depiction of the propagation of the two converging beams exiting the machined diagonal cores. A trapped cell is depicted in the overlapping area.

Optics EXPRESS

Different mirror angles (θ), larger than the critical angle of 64.79°, lead to different beam propagation angles (θ_{prop}) and thus different trapping distances (d_{trap}). These angles are shown in Fig. 1(b) and Fig. 2 shows theoretical NA and d_{trap} (lines) and experimental values of d_{trap} for three different fabricated mirror angles of 67.5°, 68° and 70° (dots). For a mirror of 67.5° the calculated NA of our system is

$$NA = n_m \sin(\varphi) = 1.039 \quad (1)$$

where n_m is the refractive index of the surrounding water (1.33) and φ is the angle of beam propagation with respect to the fiber axis as shown in Fig. 1(b), calculated using geometrical optics to be 51.4°. For these parameters, the trapping distance d_{trap}, is calculated to be 25.9 µm.

The experimental values of the trapping distance include an error, due to the resolution of the CCD camera that imaged the experimental process, as defined from the calibration of the system.

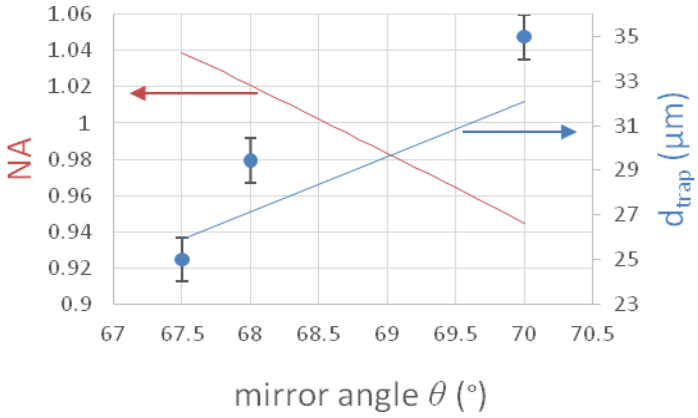

Fig. 2. Numerical evaluation of trapping distance d_{trap} (blue line) and numerical aperture NA (orange line) for a variety of mirror angles θ that are subsequently fabricated and experimentally tested. Experimentally observed trapping distances for yeast cells shown as blue circles. For 68° and 70° these are observed to have longer d_{trap} than the theoretically predicted, due to lower NA that results in an increased on-axis scattering force. The experimental trapping distances have been measured using the images captured from the CCD camera of the microscope. The resolution of this optical system leads to an error equal to 1 µm. Additionally, in the theoretical model we have not accounted for divergence which leads to a larger overlap region.

We note at this point that higher NAs may be achieved by coating the mirrored surface with metal to allow a greater range of mirror angles unrestricted by the critical angle of 64.79°. However, we have observed detrimental heating using fibers coated in metal due to absorption of the 975 nm tweezing beam, and we choose to avoid this approach.

2.2 Beam steering mirror fabrication

FIB machining was used to fabricate the mirrors on the end-face of the MCF, as seen in Fig. 3(a). The spatial precision of this machining process is on the scale of tens of nanometers. To prevent electrostatic charging during the machining process the surface of the fiber was coated with a 200 nm gold layer. The ion beam removed material from a region of 18 µm by 18 µm at the two diagonally opposite cores using a 7 nA ion current. These dimensions were chosen to cover the core diameter (8 µm) and the surrounding cladding regions. The depth of the mirror slot was 40 µm to achieve a mirror angle of 67.5 °.

Optics EXPRESS

During mirror fabrication, the rate of material removal by FIB was 3240 μm^3 h^{-1}, and the total time needed for the machining of one mirror was two hours. After fabrication the gold layer was removed in the region between the two mirrors, which can be clearly seen in Fig. 3(b), to avoid absorption of the trapping beam as it exits the fiber.

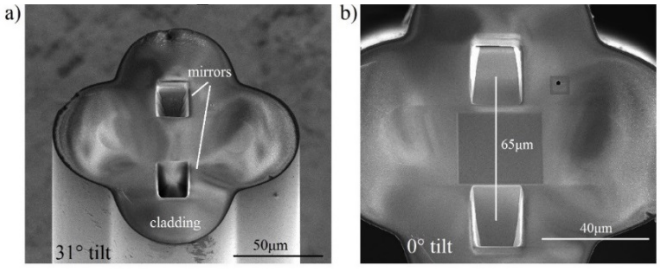

Fig. 3. a), b) Scanning electron microscope (SEM) micrographs of fiber surface after mirror fabrication on two diagonally opposite cores, when the fiber end-face is tilted in 31° and 0° with respect to the SEM, respectively. b) A dark square in the centre of the fiber can be seen and it is due to the gold layer removal using the FIB, in order to eliminate the heating effect through the trapping experiment.

2.3 Beam characterization and simulation

Two 975 nm laser diodes with maximum output power 330 mW (Thorlabs, PL980P330J, and controller CLD1015) are coupled independently into core 1 and core 2 of the MCF via a fan-out device [23]. Four single-core fibers were etched using HF acid and they were glued to align with the MCF cores. The output MCF of the fan-out is then fusion spliced to the machined fiber. Using this, each of the MCF cores can be connected to a laser diode allowing the power in each core to be independently varied. The lateral losses due to splicing, for a 1 μm misalignment is 0.532dB (11%).

Beam profile measurement was performed with the fiber placed in water, in a set up that included a water tank, a CCD camera and a micro- translation stage that was able to move in x, y, z axes as well as rotating about the vertical axis.

The rotation axis was used to determine the propagation direction relative to the fiber axis. One unmachined core in the MCF, with a circular output beam spot, was used as a position reference on the camera to show the fiber axis. With the camera held stationary, the fiber was rotated by an angle φ, as defined in Fig. 1(b), until the beam from the machined mirror was imaged. For a fiber of mirror angle 67.5°, the angle φ was measured to be 52.31°**.** Starting from this angle we calculated the corresponding θ_{prop} to be 37.69° and d_{trap} to be 25.19 μm.

Thereafter, the beam spot cross-sections from the two machined cores were captured by camera, at different distances from the fiber-end, to obtain the divergence angles. For core 1 the beam divergence was measured to be 4.42° and for core 2 the divergence was 6.52°.

Using experimental measurements of beam intensity, direction and divergence for 67.5° mirror angles, a simulation for the propagation assuming Gaussian beams can be generated using MatLab, as shown in Fig. 4(a). For comparison, Fig. 4b shows a micrograph of the MCF fiber and the propagation of the two beams in water containing yeast cells. The scattered light from the trapped cell can be clearly seen in Fig. 4b. From the simulation, the overlap region is between 15 and 30 μm away from the fiber-end, and according to theory, as shown in Fig. 2, the trapping distance should be within this range (d_{trap} = 25.9 μm for 67.5° mirrors). The trapping distance away from the fiber-end in this experiment, as it can be seen in Fig. 4(b), was 25 μm, so the difference between this value and theory was 3.5%.

Optics EXPRESS

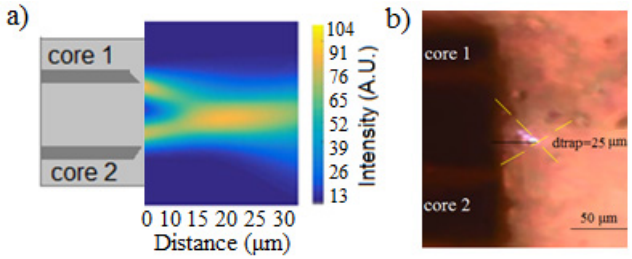

Fig. 4. Beam propagation for the two machined, diagonally opposite cores as seen from the cross-section of the multicore fiber. a)Matlab simulation of the beam propagation from the two cores. The overlapping 'trapping' area can be clearly seen when the two weakly diverging beams cross. b) Optical image of yeast cell. Core 1 and core 2 are annotated on the image and the laser light scattered by the yeast cells indicates the beam propagation angle.

3. Machined MCF-based optical tweezing

3.1 Experimental setup

The fiber tweezer was used to trap and move 7 μm diameter yeast cells in water. The experimental set up, illustrated in Fig. 5, consists of two micro-translation stages both moving in x, y and z; one is for alignment of the single fiber tweezer and the other is the laser-machined sample holder [24]. A microscope objective of × 10 magnification and a CCD camera were used for imaging a large field of view of the sample.

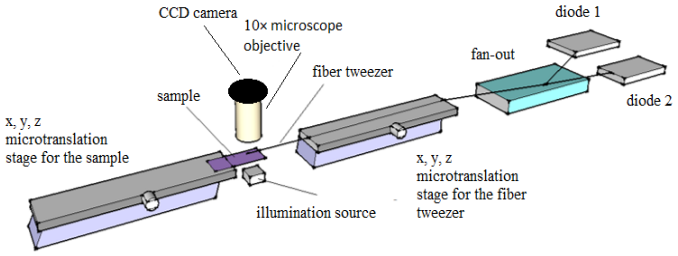

Fig. 5. Experimental set-up for using the machined MCF-based optical tweezer.

The total trapping power emitted from the MCF in the sample did not exceed 30 mW. The total power has been measured by first cleaving perpendicularly the fiber-end in order to capture all light exiting the cores. For this reason, the exact power coming out of the fabricated cores may slightly vary due to potential scattering inside the sample medium. The two 975 nm laser diodes and the fan-out are the same as those described in section 2.3.

Yeast cells were suspended in water and experiments performed at room temperature. With light in only one of the cores there was obvious movement of the cells that entered the beam along the direction of beam propagation (Visualization 1). When both diodes were turned on, single cells were trapped at a point 24-27 μm away from the fiber-end and at approximately 0.6 mm above the bottom of the sample. The x axis is defined as the axis parallel to the fiber axis, the y axis as perpendicular to the fiber axis and z as the axis that runs up and down through the sample. Trapping was confirmed in 3 dimensions by moving the fiber and the sample in the x, y and z directions with defined speed between 0.05 and 0.08 mm s^{-1} (Fig. 6, Visualization 2).

In Fig. 6(a)-6(c), the sample is moved up and down along the z axis. The fiber and the trapped cell remain in focus while background cells move out of focus. In Fig. 6(d)-6(f) and Fig. 6(g)-6(i), the fiber is moved along the x axis and y axis, respectively, while the sample is stationary. The cells in the surrounding medium change position with respect to the fiber-end

Optics EXPRESS

due to flow created when translating the fiber. In contrast, the trapped cell remains at the same distance from the fiber-end.

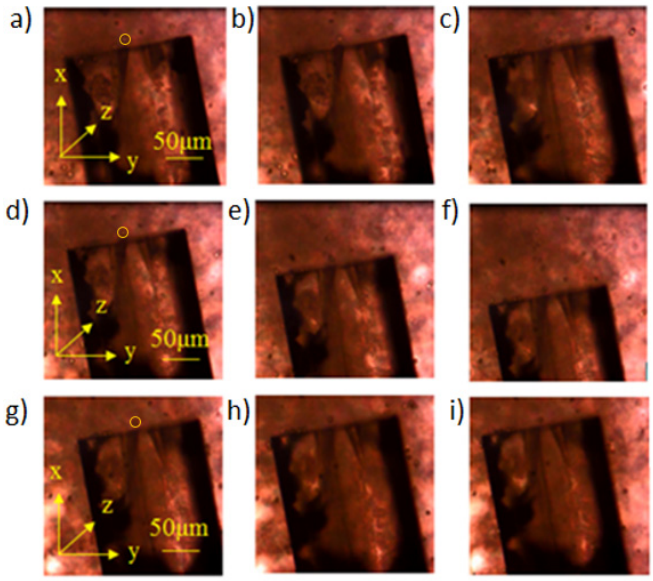

Fig. 6. Trapped yeast cell using 4.9 mW and 17.2 mW optical power from core 1 and 2 respectively. a)-c) Movement in z axis d)-f) movement in x axis and g)-i) movement in y axis. The trapped particle is shown inside the yellow circle.

3.2 MCF- based tweezer characterisation

To calculate the force exerted on the cell by the fiber tweezer (F_{fiber}), we used a conventional optical tweezer (OT) to determine the force required to overcome the MCF-based tweezer. The OT is based on a 976 nm diode laser focused by a microscope objective lens of × 60 magnification and NA of 0.90. A cell was trapped by the fiber tweezer using a maximum total optical power of 30 mW (the combined power of core 1 and core 2) and the OT was aligned orthogonal to the fiber axis, so that its beam centre was ~5-7µm away from the fiber-trapped cell. The OT was turned on and the power gradually increased until the cell was pulled out of the fiber trap into the OT. The OT trapping force (F_{trap}) was pre-calibrated by equating to Stokes' drag force (F_{drag}). The calibration was performed by measuring the critical trapping velocity (υ_c) for a variety of OT powers and calculating Stokes' drag force,

$$F_{drag} = 6\pi\eta r\upsilon_c \tag{2}$$

where the viscosity, η of water is 8.9×10^{-4} Pa and the trapped particle radius, r, is on average 3.5 µm [25]. The instant that the fiber trap is broken by the OT, F_{fiber} is equal to F_{trap}. This is performed for fiber-trap powers between 6- 30 mW and is repeated for 4-5 times for different cells for each power. OT powers in the range of 0.2 mW to 0.4 mW were sufficient to break the fiber trap. The force of the fiber trap at different powers was calculated and is shown in Fig. 7.

Optics EXPRESS

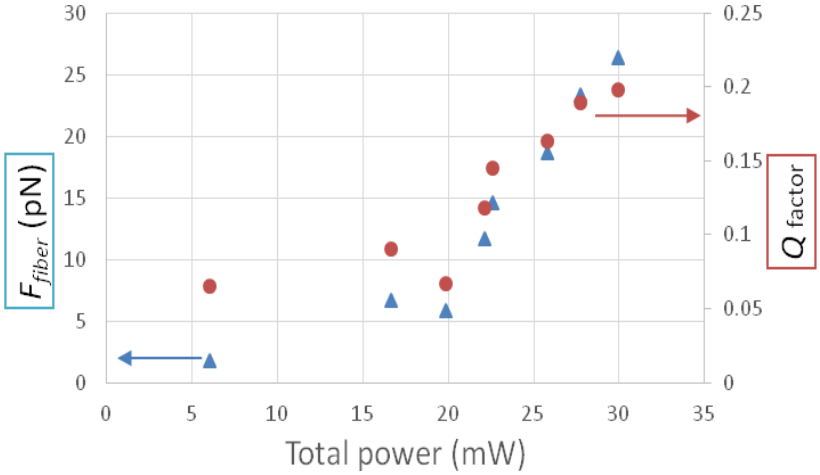

Fig. 7. Blue triangles: Experimental values of the fiber force (F_{fiber}) which were calculated by equating the trapping force of the OT (F_{trap}) that broke the fiber trap. Orange circles: The efficiency factor Q for different total powers of the tweezing probe.

The results for F_{fiber} for this MCF-based tweezer are in broad agreement with other optical fiber traps [21], [26] that reported forces between 0.5 pN and 5 pN for powers of 0.5 mW to 5 mW, and slightly weaker than conventional OT that report forces up to 35 pN for powers up to 80 mW [27].

The dimensionless trap efficiency parameter, Q,can be estimated using the total fiber trapping power values and the calculated force. For fiber trapping power, P, the refractive index of the water n = 1.33 and c the speed of light in a vacuum, then Q, for this particular fiber tweezer with machined mirrors of 67.5°, is given by [26]

$$Q = \frac{F_{fiber}c}{nP} \tag{3}$$

Previous studies quoting the trapping efficiency parameter of a fiber-based tweezing system, present values of Q = 0.2 [26] or lower; for example Q = 0.1, as reported by Yu *et al.* in their study [28]. The trapping efficiency parameter of a microscope-based OT is slightly higher with values between 0.10 to 0.570 [27], [29], [30]. This difference between the two types of tweezing systems can be explained due to the NA of the fiber-based system (in this case 1.039) which is lower than an OT (typically 1.3), so the light is not focused as tightly as in conventional OT.

Optical trapping using the MCF-based tweezer is analogous to trapping using a Laguerre-Gaussian (LG) [31] beam in conventional microscope-based OT. The LG profile is such that the on-axis intensity is zero, hence the optical trap is stronger because there is no on-axis scattering force to push the particle out of the trap in the direction of beam propagation [32]. In a similar manner, our MCF design has no on-axis rays contributing to a scattering force along the direction of the fiber axis. In addition, and in contrast to the conventional tightly focused beam of OT, the beams emitted here are slightly diverging, so the intensity is approximately 0.0379 × 10^6 W/cm^2 which is significantly lower than OT (approximately 4.53 × 10^6 W/cm^2) and so optical and thermal damage due to trapping is minimised.

3.3 Raman spectroscopy for yeast cells

The MCF-based tweezer was designed to be portable and at the same time to hold and manipulate a cell under a microscope without the need to modify the microscope system. Additionally, it can hold and manipulate the trapped cell away from any substrate. One major

issue related to single cell Raman spectroscopy is the background signal of the substrate (microscope slide) which dominates the Raman signal. In addition to this, any fluid flow in the sample leads to an uncontrollable movement of the cell in suspension making spectroscopy difficult, particularly if long integration times are required to analyze the cell or particle. Ideally, it is desirable to hold the cell under test in a stable position some distance away from the substrate.

Optically trapping cells in a stable position to perform Raman spectroscopy has been reported elsewhere [33], where a single cell could be trapped by the focused Raman laser beam. However, this approach restricts the ability to manipulate the cell and change its position below the microscope. To address this, a trap of two counter-propagating beams formed from two opposed fibers has been demonstrated to stably hold and manipulate the cell below the Raman microscope, but limitations arise from the restricted space to set up this trapping system, the alignment required and the difficulty in flowing desired cells into the trap [6]. Our MCF-based tweezer circumvents these issues. This is demonstrated using a commercial unmodified Raman microscope (Renishaw InVia). A × 50 objective with a NA of 0.75 was used to focus the Raman excitation beam, of 785 nm wavelength and power of 92 mW. The spot diameter was calculated using the Rayleigh criterion to be 1.27 μm and spectral acquisition time was 10 seconds in all experiments.

Both live and dead yeast cells have been trapped using the MCF-based tweezer to acquire the Raman spectra, as shown in Fig. 8.

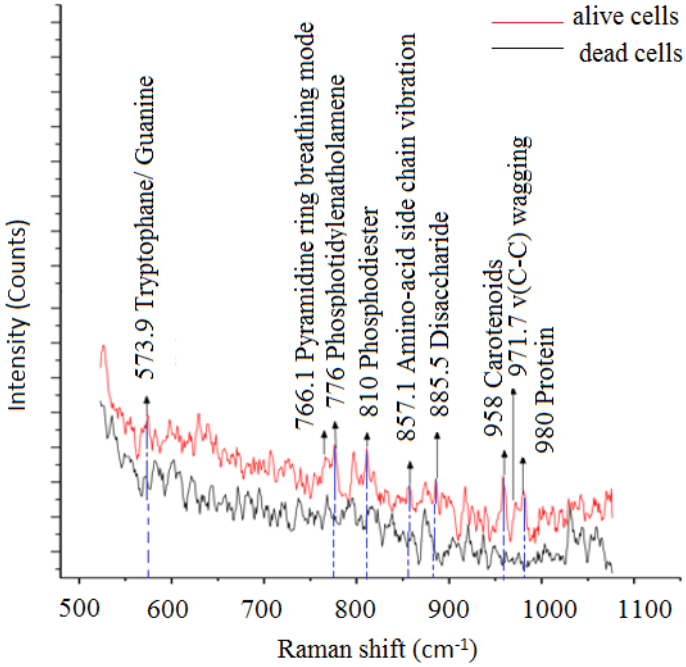

Fig. 8. Comparison between the spectra of dead (black spectrum) and live (red line) yeast cells. The main differences appear in peaks that define proteins and DNA structures. Blue dashed lines indicate the signals that appear in the live cell spectra but vanish or are reduced in intensity in the dead cell spectra. These are representative spectra from a single live cell and a single dead cell.

It is often difficult to discriminate live from dead cells through optical observation alone due to their similar morphology, however Fig. 8 shows that the main differences in Raman spectra between live and dead yeast cells appear in DNA components and proteins peaks. In

Optics EXPRESS

live cells (red spectrum) these peaks appear more intense than in case of dead cells (black spectrum), due to protein and nucleic acids denaturation and degradation in the dead cells [34]. We have observed that the intensity of the Raman signal increases with increasing fiber tweezer power. This enhancement in Raman signal from a trapping beam has been reported by others [13].

4. Conclusions

We have designed, fabricated and demonstrated a flexible and portable single fiber optical tweezer. The fiber tweezer is based upon a multicore fiber containing two micro-machined mirrors directing two emitted beams to cross a short distance from the end of the fiber. Yeast cells have been stably trapped and manipulated in x, y and z and held under a Raman probe beam in order to obtain spectra from live and dead cells, eliminating the detrimental background signals and flow effects. The MCF-based tweezer has a maximum NA of 1.039, for 67.5° mirror angle, and can exert a maximum trapping force of 26.5 pN, as measured using well-characterized, orthogonally directed, conventional optical tweezers. Finally, the quality, Q of this particular fiber trap was calculated to be between 0.067 and 0.198, in line with conventional optical tweezers, but allowing more flexibility in the type of trapping and imaging experiments that can be performed.

Funding

The Royal Society Paul Instrument Fund; Renishaw-Heriot Watt alliance funds; EPSRC Equipment Fund EP/J015040/1; Heriot-Watt University Institute of Photonics and Quantum Science studentship.

Acknowledgments

The authors thank Renishaw plc for the kind gift, to the School of Engineering and Physical Sciences, Heriot-Watt University, of the Renishaw InVia Spectrometer.